J. Fluid Mech. (1986), *vol.* 167, *pp.* 465–479
Printed in Great Britain

Resonant sloshing in shallow water

By H. OCKENDON, J. R. OCKENDON AND A. D. JOHNSON

Mathematical Institute, Oxford University, 24–29 St. Giles,
Oxford OX1 3LB, UK

(Received 23 August 1985)

The ordinary differential equation

$$\tfrac{1}{3}\kappa^2(g''+g)-\lambda g-\tfrac{3}{2}g^2+\frac{2}{\pi}\cos t=-\frac{3}{2}\int_{-\pi}^{\pi}g^2\,\mathrm{d}t,$$

which represents forced water waves on shallow water near resonance, is considered when the dispersion κ is small. Asymptotic methods are used to show that there are multiple solutions with period 2π for a given value of the detuning parameter λ. The effects of dissipation are also considered.

1. Introduction

The study of the effects of nonlinearity on the resonant sloshing of water in a horizontally oscillated container was initiated by Moiseyev (1958) who only considered situations where the water is fairly deep. Other authors (Chester 1968; Ockendon & Ockendon 1973; Cox & Mortell 1983; Miles 1985) have since suggested that, for shallow water, the periodic response near one of the resonant frequencies is governed by a certain second-order non-autonomous ordinary differential equation. When the depth is formally set equal to a critical depth, which is zero in the absence of surface tension, and when damping is neglected, this ordinary differential equation reduces to a quadratic equation which has a unique continuous solution outside a small detuning range close to a resonant frequency. The same quadratic equation is encountered in the resonant oscillations of gas in a tube (Chester 1964) in which case there is a unique solution for all values of the detuning parameter, but the solution contains a compressive shock wave in the detuning range mentioned above. However, apart from the experimental evidence of Chester & Bones (1968) and the numerical results of Ockendon & Ockendon (1973), Chester (1968) and Cox & Mortell (1986), little is known about the effects of a small dispersive term, representing the depth, on these resonant responses. The aim of this paper is to describe some asymptotic solutions which may help to understand the *multiple* periodic solutions which the above authors have described.

In §2 we shall give a brief rederivation of the governing ordinary differential equation and recapitulate its behaviour in the non-dispersive case. Then in §3 we shall describe asymptotic representations of the periodic response for small non-zero water depth. In the final section we discuss how dissipative effects modify the results of §3.

2. A model for shallow-water sloshing

Following Ockendon & Ockendon (1973), we begin by assuming that two dimensional inviscid irrotational motion is induced in a rectangular tank of water of length πL which is forced to oscillate horizontally with frequency ω and amplitude a, where

$a \ll L$, and look for solutions with period $2\pi/\omega$ in time. We shall also neglect surface tension initially although we shall return to real-fluid effects later.

Choosing the x-axis along the mean surface elevation hL above the base, the dimensionless model for the velocity potential $\epsilon\phi$ and the elevation $\epsilon\eta$ is

$$\nabla^2\phi = 0 \quad \text{in } -\epsilon\cos t < x < \pi - \epsilon\cos t, \quad -h < y < \eta,$$

with

$$\left.\begin{aligned} &\phi_y = 0 \quad \text{on } y = -h, \\ &\phi_y = \eta_t + \epsilon\phi_x\eta_x \\ &\eta + (1+\delta)\tanh h(\phi_t + \tfrac{1}{2}\epsilon(\phi_x^2+\phi_y^2)) = 0 \\ &\phi_x = \sin t \quad \text{on } x = -\epsilon\cos t,\ \pi - \epsilon\cos t, \end{aligned}\right\} \text{ on } y = \epsilon\eta,$$

where $\epsilon = a/L$ and the detuning $\delta = -1 + L\omega^2\coth h/g$ is small near the fundamental resonant frequency. For shallow water we have three small parameters, ϵ which measures the drive amplitude, δ the detuning parameter, and h the depth parameter. As explained in Ockendon & Ockendon (1973) the appropriate parameter ranges, which match those of Moiseyev (1958) when $h = O(1)$, are the 'Korteweg–de Vries' scalings in which

$$\kappa = h\epsilon^{-\frac{1}{4}}, \quad \lambda = \delta\epsilon^{-\frac{1}{2}}$$

are both $O(1)$. Since h is small ($O(\epsilon^{\frac{1}{4}})$), it is necessary to rescale by writing $y = \epsilon^{\frac{1}{4}}\bar{y}$, $\phi = \epsilon^{-\frac{1}{2}}\bar{\phi}$ and $\eta = \epsilon^{-\frac{1}{4}}\bar{\eta}$ so that the equations become

$$\bar{\phi}_{\bar{y}\bar{y}} + \epsilon^{\frac{1}{2}}\bar{\phi}_{xx} = 0,$$

with

$$\left.\begin{aligned} &\bar{\phi}_{\bar{y}} = 0 \quad \text{on } \bar{y} = -\kappa, \\ &\bar{\phi}_{\bar{y}} = \epsilon^{\frac{1}{2}}\bar{\eta}_t + \epsilon\bar{\phi}_x\bar{\eta}_x \\ &\bar{\eta} + \kappa(1+\lambda\epsilon^{\frac{1}{2}})(1-\tfrac{1}{3}\kappa^2\epsilon^{\frac{1}{2}}+\ldots)(\bar{\phi}_t + \tfrac{1}{2}\bar{\phi}_{\bar{y}}^2 + \tfrac{1}{2}\epsilon^{\frac{1}{2}}\phi_x^2) = 0 \\ &\bar{\phi}_x = \epsilon^{\frac{1}{2}}\sin t \quad \text{on } x = -\epsilon\cos t, \quad \pi - \epsilon\cos t. \end{aligned}\right\} \text{ on } \bar{y} = \epsilon^{\frac{1}{2}}\bar{\eta},$$

Now expand $\bar{\phi} = \phi_0 + \epsilon^{\frac{1}{2}}\phi_1 + \epsilon\phi_2 + \ldots$ and $\bar{\eta} = \eta_0 + \epsilon^{\frac{1}{2}}\eta_1 + \epsilon\eta_2 + \ldots$. The terms of $O(1)$ give

$$\phi_0 = A(x,t), \quad \eta_0 = -\kappa A_t,$$

where

$$A_x = 0 \quad \text{on } x = 0,\ \pi.$$

The next approximation gives $\phi_{1\bar{y}\bar{y}} = -A_{xx}$ and, using the condition on $\bar{y} = -\kappa$, $\phi_1 = -\frac{1}{2}A_{xx}(\bar{y}+\kappa)^2 + C(x,t)$. On $\bar{y} = 0$, $\phi_{1\bar{y}} = \eta_{0t}$, which gives $A_{xx} = A_{tt}$ and hence $\phi_0 = f(t-x) + f(t+x)$, where the conditions on $x = 0, \pi$ imply that f has period 2π. The third boundary condition leads to

$$\eta_1 = \tfrac{1}{2}\kappa^3 A_{xxt} - \kappa C_t - \kappa\lambda A_t - \tfrac{1}{2}\kappa A_x^2 + \tfrac{1}{3}\kappa^3 A_t.$$

Pursuing the solution to terms of $O(\epsilon)$,

$$\phi_{2\bar{y}} = \tfrac{1}{6}A_{xxxx}(\bar{y}+\kappa)^3 - C_{xx}(\bar{y}+\kappa)$$

and the boundary condition becomes

$$\phi_{2\bar{y}} = \eta_{1t} + \phi_{0x}\eta_{0x} - \eta_0\phi_{1\bar{y}\bar{y}} \quad \text{on } \bar{y} = 0.$$

Hence

$$\begin{aligned} C_{xx} - C_{tt} &= -\tfrac{1}{3}\kappa^2 A_{xxxx} + \left(\lambda - \frac{\kappa^3}{3}\right)A_{xx} + A_t A_{xx} + 2A_x A_{xt} \\ &= -\tfrac{1}{3}\kappa^2(f_+^{\mathrm{iv}} + f_-^{\mathrm{iv}}) + (\lambda - \tfrac{1}{3}\kappa^2)(f_+'' - f_-'') + (f_+' + f_-')(f_+'' + f_-'') + 2(f_+' - f_-')(f_+'' - f_-''), \end{aligned}$$

where

$$f_\pm = f(t \pm x)$$

and $C_x = \sin t$ on $x = 0, \pi$. Solving this problem for $C(x,t)$ and using the assumption that the solution has period 2π in t gives

$$\tfrac{1}{3}\kappa^2 f^{\mathrm{iv}}(t) - (\lambda - \tfrac{1}{3}\kappa^2) f''(t) - 3f'(t)f''(t) = \frac{2}{\pi}\sin t$$

or, writing $f' = g$ and integrating once,

$$\tfrac{1}{3}\kappa^2(g'' + g) - \lambda g - \tfrac{3}{2}g^2 = -\frac{2}{\pi}\cos t + \text{constant}, \tag{1}$$

where the periodicity of f implies that g has period 2π and zero mean over the interval $(-\pi, \pi)$. It is convenient to write $g = -\frac{1}{3}\lambda + G$ and then the equation is

$$\kappa^2(G'' + G - \tfrac{1}{3}\lambda) = \frac{9}{2}\left(G^2 - \frac{4}{3\pi}(\cos t + c)\right), \tag{2}$$

where G has period 2π,

$$\int_{-\pi}^{\pi} G\,\mathrm{d}t = \tfrac{2}{3}\pi\lambda \quad \text{and} \quad c = \tfrac{3}{8}\int_{-\pi}^{\pi} G^2\,\mathrm{d}t.$$

The elevation of the surface $\epsilon\eta$ is $\kappa\epsilon^{\frac{2}{3}}(\frac{2}{3}\lambda - G(t-x) - G(t+x))$.

If the Reynolds number $\omega l^2/\nu = O(\epsilon^{-\frac{3}{2}})$, the effect of a viscous boundary layer on the bottom is significant and introduces a Laplace convolution of g and $t^{-\frac{1}{2}}$ into (1) as explained in Chester (1968). This leads to a difficult integro-differential equation for g, and a more tractable model for damping is to introduce a term $\mu g'(t)$ into the left-hand side of (1) to represent the viscosity of the fluid. A small surface tension γ can be added to the model and, assuming the contact angle remains close to $\frac{1}{2}\pi$, merely changes the coefficient κ^2 in (2) to $(\kappa^2 - \sigma)$ where $\sigma = 3\gamma\epsilon^{-\frac{1}{2}}/\rho g L^2$ [Vanden-Broeck 1984]. The critical depth for no dispersion is $(3\gamma/\rho g)^{\frac{1}{2}}$. Three-dimensional effects would be harder to incorporate and no attempt to do so is made in this paper.

There are two situations in which the relevant solutions of (1) or (2) can be described quite easily. First, when $\kappa \to \infty$ with $\lambda\kappa^{\frac{2}{3}} = O(1)$, a simple rescaling retrieves the shallow-water limit of Moiseyev's (1958) solution. This 'Duffing-like' response was described by Ockendon & Ockendon (1973), who also showed that as $\kappa \to \infty$ with $\lambda\kappa^{-2} = O(1)$ other periodic solution branches can occur. In both these cases, in the absence of damping, the amplitude on some solution branches can increase indefinitely as a suitably scaled detuning becomes large; as with Duffing's equation these solution branches join up with solutions of the fully nonlinear problem where $\epsilon = O(1)$. Secondly, when $\kappa = 0$, equation (2) reduces to the algebraic equation

$$G^2 = \frac{4}{3\pi}(\cos t + c), \tag{3}$$

whose solution, including small viscosity, has been discussed by Chester (1964) in connection with organ-pipe resonances. Solutions of (3) are continuous if $c \geqslant 1$, which gives $|\lambda| \geqslant (96/\pi^3)^{\frac{1}{2}} = \lambda_*$, say; these solutions are sketched in figure 1 (*a*). However, if $|\lambda| < \lambda_*$ the solutions involve compressive shocks as shown in figure 1 (*b*), and in this detuning range the value of c is frozen at 1.

The birth of a shock wave when λ is near λ_* can be seen by balancing the small viscous term $\mu G'$ against the forcing term near $t = \pi$. Writing $t = \pi + \tau\mu^{\frac{1}{2}}$, $c = 1 + \mu\bar{C}$, $G = \mu^{\frac{1}{2}}\bar{G}$, we obtain

$$\bar{G}_\tau = \frac{9}{2}\left(\bar{G}^2 - \frac{2}{3\pi}\tau^2 - \frac{4}{3\pi}\bar{C}\right), \tag{4}$$

where, in order to match with the separatrix in figure 1, $\bar{G} \sim (2/3\pi)^{\frac{1}{2}}|\tau|$ as $|\tau| \to \infty$.

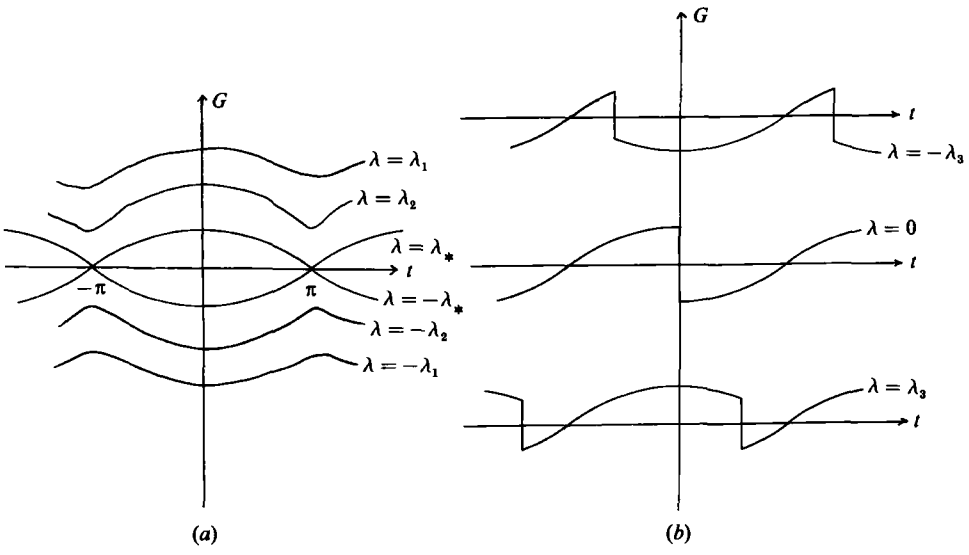

FIGURE 1. (*a*) Continuous solutions of (3) for $\lambda = \pm\lambda_1, \pm\lambda_2, \pm\lambda_*$, where $\lambda_1 > \lambda_2 > \lambda_* > 0$. (*b*) Discontinuous solutions of (3) for $\lambda = \pm\lambda_3, 0$, where $0 < \lambda_3 < \lambda_*$.

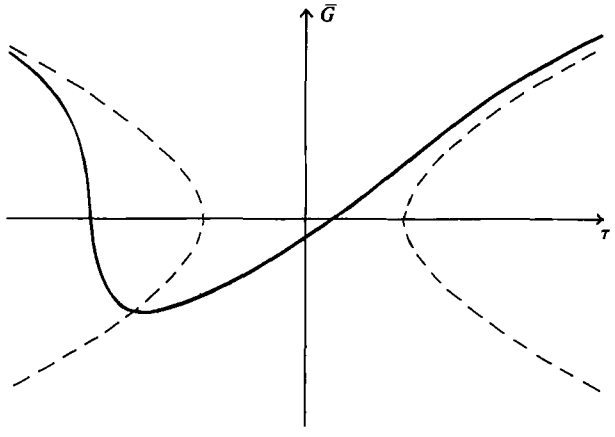

FIGURE 2. The birth of a shock: – – –, curve on which $G_\tau = 0$; ——, solution of (4) where $-(\pi/54)^{\frac{1}{2}} < \bar{C} < 0$.

It can be shown by a shooting argument that when $\bar{C} > -(\pi/54)^{\frac{1}{2}}$, the unique solution for which $\bar{G} \sim (2/3\pi)^{\frac{1}{2}}\,\tau$ as $\tau \to \infty$ tends to $-(2/3\pi)^{\frac{1}{2}}\,\tau$ as $\tau \to -\infty$. However when $\bar{C} = -(\pi/54)^{\frac{1}{2}}$, $\bar{G} = (2/3\pi)^{\frac{1}{2}}\,\tau$ is this unique solution and for $\bar{C} \leqslant -(\pi/54)^{\frac{1}{2}}$ this solution does not have the required form as $\tau \to -\infty$; the solution is of the form shown in figure 2 as $\bar{C} \to -(\pi/54)^{\frac{1}{2}}$ from above.

The numerical and experimental evidence mentioned in § 1 suggests that for non-zero values of κ, multiple periodic solutions are possible for the same value of the detuning parameter λ. This evidence gives a clue to the asymptotic response for small κ, which we will describe in the next section.

3. Asymptotic solutions of (2) as $\kappa \to 0$

For $|\lambda| > \lambda_*$, (3) is the first term of a possible asymptotic expansion of a solution of (2) as $\kappa \to 0$. However, we may also seek solutions which are close to (3) except in a small region where G'' is large. In particular we can write $t = t_0 + \kappa\tau$ and neglect terms in $O(\kappa^2)$ to give

$$\frac{\mathrm{d}^2 G}{\mathrm{d}\tau^2} = \tfrac{9}{2}(G^2 - u^2(t;c)), \tag{5}$$

where we define $u(t;c) = u = +[(4/3\pi)(\cos t + c)]^{\frac{1}{2}}$. As $|\tau| \to \infty$ it is now possible for G to approach the solution $G = u$, which is slowly varying on the τ-scale and corresponds to a saddle point in the (G, G_τ)-phase plane (figure 3) when u is formally regarded as a constant. Although $G = u$ would be an unstable equilibrium point if we regarded (5) as an oscillator, this does not mean that a particular solution of (5) which tends to u for large τ cannot correspond to a physically acceptable solution of the sloshing-tank problem.

As t varies, the phase plane will slowly evolve periodically and we can construct a function G which for most of the period 2π in t will remain near u, but which has a finite number of excursions in the vicinity of the homoclinic orbit of figure 3. One such possible solution is shown schematically in figure 4.

The inner problem (5) has periodic solutions in the fast timescale τ which correspond to rapid oscillations or 'spikes' on the slow timescale t. This inner solution can be matched to the outer solution $G = u$ as $\tau \to \pm\infty$ as long as $u' = 0$, so spikes can only occur near $t = n\pi$.

Any finite number of spikes can be accommodated at $t = 0$ where u has a maximum, but at most one spike can occur at $t = \pi$ where u has a minimum value. This can be seen by considering the slowly varying phase plane of figure 3 and realizing that a periodic solution cannot escape from within the homoclinic orbit. This pattern of maxima and minima was indicated by Chester (1968), who considered equation (5) when c is close to unity. This problem has also been considered by Kath (1985) who uses an energy method to come to the same conclusion.

The introduction of one or more spikes decreases the mean value of G for a given u and so these solution branches can exist for values of $\lambda < \lambda_*$. The response diagram for some of these solutions is sketched in figure 5 where we plot

$$c\left(= \frac{3}{8}\int_{-\pi}^{\pi} G^2 \,\mathrm{d}t\right)$$

against the detuning parameter λ.

The number of spikes on a solution branch is indicated by (i, j) where i is the number of spikes at $t = 0$ and j is the number at $t = \pi$. As $c \downarrow 1$ the amplitude of the spike at $t = \pi$ decreases and there is a critical value c_0 (close to one) at which the $(i, 0)$-solution and the $(i, 1)$-solution coincide.

Starting from the $(i, 0)$-branch at $c = c_0$ and then increasing c we can see the 'birth' of the spike at $t \approx \pi$ by considering a local analysis of (2). Putting $t = \pi + \kappa^{\frac{2}{3}}\tau$, $c = 1 + \kappa^{\frac{4}{3}}\bar{c}$, $G = \kappa^{\frac{2}{3}}\bar{G}$ leads to the equation

$$\bar{G}_{\tau\tau} = \frac{9}{2}\left(\bar{G}^2 - \frac{2}{3\pi}\tau^2 - \frac{4}{3\pi}\bar{c}\right), \tag{6}$$

which may be compared with equation (4). As in §2, we require solutions of (6) satisfying $G \sim (2/3\pi)^{\frac{1}{2}}|\tau|$ as $|\tau| \to \infty$. Now the arguments of Holmes & Spence (1984)

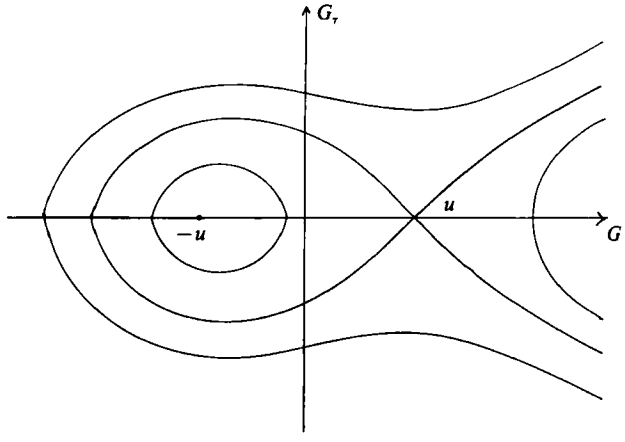

FIGURE 3. Sketch of phase plane for equation (5).

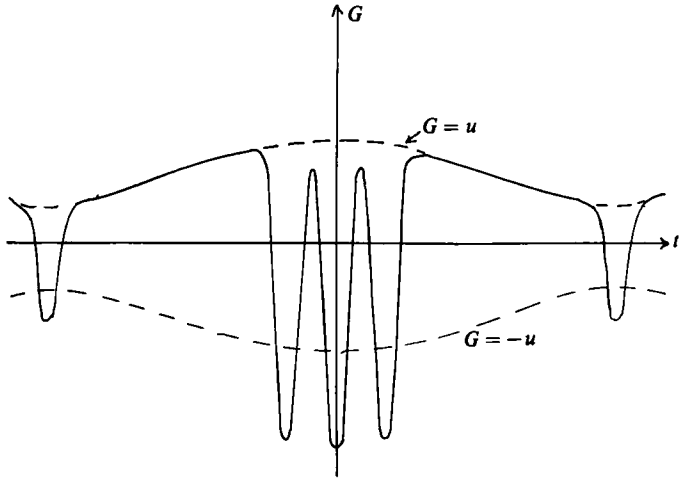

FIGURE 4. A possible 'spiked' solution.

suggest there are at least two symmetric solutions of this type if $\bar{c}$ is positive, and comparison arguments suggest that there are no solutions of this type if $\bar{c}$ is large and negative. We therefore carried out numerical experiments to test the hypothesis that there are exactly two symmetric solutions with the correct asymptotic behaviour for $\bar{c}$ greater than a critical value $\bar{c}_0 < 0$, and that these solutions coincide for $\bar{c} = \bar{c}_0$. A numerical method (NAG D02BBF) was used to solve (6) with $G(0) = \alpha$ and $G'(0) = 0$. The value of α was varied and the criterion used for an acceptable solution was as follows; either

(i) when a value α_+^* of the shooting parameter α was found such that the solution for $\alpha = \alpha_+^* + 10^{-2}$ appeared to become unbounded for finite τ and yet the solution for $\alpha = \alpha_+^* - 10^{-2}$ had zero slope for finite τ, or

(ii) when a negative value α_-^* of α gave the same behaviour with $\alpha = \alpha_-^* \mp 10^{-2}$ respectively.

For large positive $\bar{c}$, unique values of $\alpha_\pm^*$ were found, and as $\bar{c}$ was decreased α_+^* decreased and α_-^* increased until the two values coincided at the critical value

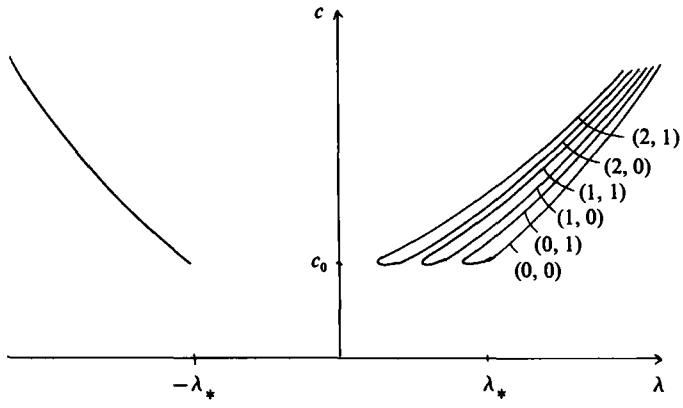

FIGURE 5. Response diagram for spiked solutions.

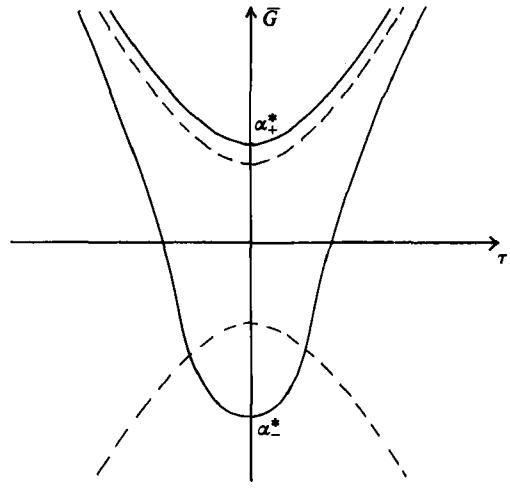

FIGURE 6. Solutions of (6) when $\bar{c} > \bar{c}_0$. The dotted curves are the loci of points where $\bar{G}_{\tau\tau} = 0$.

$\bar{c}_0 \approx -0.45$. The two solutions for $\bar{c} > \bar{c}_0$ are sketched in figure 6. As $\bar{c}$ increases the lower branch will develop into the solution with a spike at $t = \pi$.

An estimate of the time taken to complete a spike can be made since most of the time is spent near the saddle point $G = u$ and is proportional to $\kappa \log \kappa / u^{\frac{1}{2}}$ (Kath 1985). Thus as $c \to +\infty$ the duration of the spikes approaches zero and the mean value of each solution approaches that of the basic solution u as shown by the bunching of the response curves for large λ in figure 5.

When the number of spikes becomes large the oscillations will no longer be close to the homoclinic orbit, but we can exploit the fact that they occur on a fast timescale and use the method of adiabatic invariance or multiple scales. We introduce a fast time $\xi = f(t)/\kappa$ and write (2) in terms of the two timescales t, ξ to obtain

$$f'^2 G_{\xi\xi} + \kappa(f'' G_\xi + 2f' G_{\xi t}) + \kappa^2(G_{tt} + G - \tfrac{1}{3}\lambda) = \tfrac{3}{2}(G^2 - u^2).$$

Then we expand $G = G_0 + \kappa G_1 + \ldots$ and choose $f(t)$ so that $G_0, G_1 \ldots$ have the same constant period Ω in ξ, which will ensure that the expansion is uniformly valid as

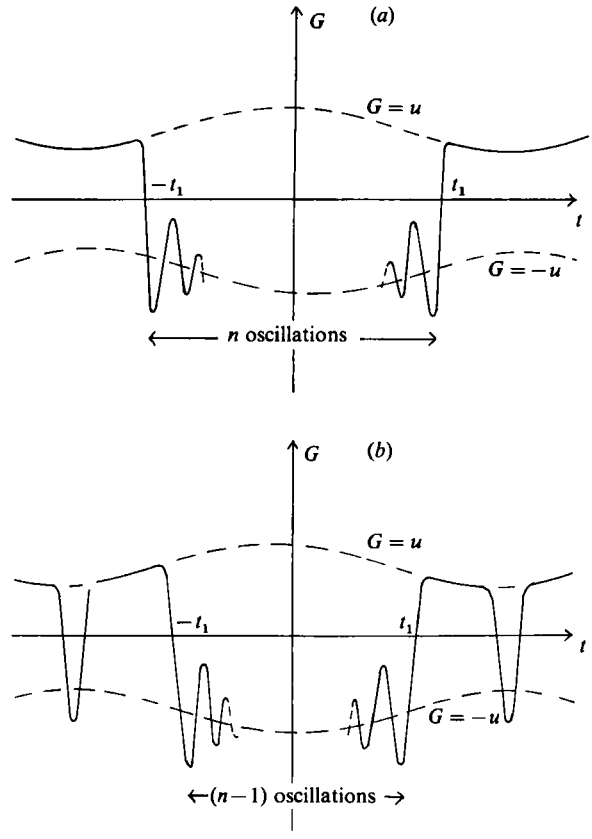

FIGURE 7. Solutions which oscillate about $G = -u$.

$|\xi| \to \infty$. For details of this method see Luke (1966) or Kuzmak (1959). The equation for G_0 is

$$f'^2 G_{0\xi\xi} = \tfrac{9}{2}(G_0^2 - u^2), \tag{7}$$

whose phase plane is shown in figure 3. From the equation for G_1 and the periodicity condition we obtain

$$f' \int_0^{\Omega} G_0^2 \, \mathrm{d}\xi = K, \tag{8}$$

where K is some constant. This relation implies that the area within a periodic solution in the $(G_0, G_{0\xi})$-phase plane is $K/f'(t)$. For all oscillatory solutions of (7) except those close to the homoclinic orbit, the period in ξ is close to $2\pi f'/3u^{\frac{1}{2}}$ and hence we need to choose $f' = 3u^{\frac{1}{2}}$. This gives the amplitude of small oscillations about $-u(t)$ as

$$\left[\int_0^{\Omega} G_{0\xi}^2 \, \mathrm{d}\xi \right]^{\frac{1}{2}} = \frac{K^{\frac{1}{2}}}{3^{\frac{1}{2}} u^{\frac{1}{4}}}. \tag{9}$$

Thus there will be solutions of the form sketched in figure 7(*a*) where the amplitude of oscillations decreases and increases as $u(t)$ increases and decreases respectively.

It will also still be possible to have solutions with a single spike at $t = \pm\pi$, together

with a band of oscillations symmetrical about $t = 0$, as shown in figure 7 (*b*). For a solution of the type shown in figure 7,

$$\tfrac{2}{3}\pi\lambda = \int_{-\pi}^{\pi} G\,\mathrm{d}t \sim 2\int_0^{t_1}(-u)\,\mathrm{d}t + 2\int_{t_1}^{\pi} u\,\mathrm{d}t,$$

since the contributions to the integral from the oscillations will cancel out to first order. This gives solutions with values of λ in the range $(-\lambda_*, \lambda_*)$. The period of oscillations is approximately $2\pi\kappa/3u^{\frac{1}{2}}$ on the t-scale and so as c increases the oscillations will 'bunch up' more closely about $t = 0$, and t_1 will decrease as c increases.

When the oscillations about $G = -u(t)$ have spread from $-\pi$ to π we may equally well consider the solution as a perturbation about $G = -u$ and use the WKB method on (2). This leads to a solution of the form

$$G = -u + \frac{A}{u^{\frac{1}{4}}}\cos\left(\frac{\phi_0(t)}{\kappa}\right) + O(\kappa^2), \tag{10}$$

where $\phi_0'(t) = 3u^{\frac{1}{2}}$ and A is an arbitrary small constant. This agrees with the solution of (7)–(9) when we put $A = [\frac{1}{3}K]^{\frac{1}{2}}$. The periodicity condition on G implies that $\phi_0(t+2\pi) - \phi_0(t) = 2\pi n\kappa$, where n is an integer and so

$$\int_{-\pi}^{\pi} 3(u(t;c))^{\frac{1}{2}}\,\mathrm{d}t = 2\pi n\kappa, \tag{11}$$

which determines values $c = c_n$ for which periodic solutions of the form (10) are possible. Since $c > 1$ in order that $u^{\frac{1}{2}}$ be defined for all t, there is a minimum value of n, n_1 say, for which (10) has a solution. Near $c = c_n$ and

$$\lambda = \lambda_n = -\frac{3}{2\pi}\int_{-\pi}^{\pi} u(t, c_n)\,\mathrm{d}t,$$

we write $G = -u + \bar{g}$, $c = c_n + \delta$ and $\lambda = \lambda_n + \delta\bar{\lambda}$ so that (2) is

$$\kappa^2(\bar{g}'' + \bar{g}) + 9u\bar{g} - \tfrac{9}{2}\bar{g}^2 = \kappa^2(u'' + u + \tfrac{1}{3}(\lambda_n + \delta\bar{\lambda})), \tag{12}$$

where
$$u = +\left[\frac{4}{3\pi}(c_n + \cos t + \delta)\right]^{\frac{1}{2}}.$$

When c_n is large,

$$u \sim \left(\frac{4c_n}{3\pi}\right)^{\frac{1}{2}}\left[1 + O\left(\frac{1}{c_n}\right)\right], \quad u'' \sim -\frac{\cos t}{(3\pi c_n)^{\frac{1}{2}}}$$

so that (12) can be analysed using multiple scales in exactly the same way as Duffing's equation when the natural frequency greatly exceeds the forcing frequency.† The response diagram obtained is just as for Duffing's equation as shown in figure 8.

As δ increases the number of oscillations on the upper branches in figure 8 is conserved, and the solutions first evolve into solutions of the type illustrated in figure 7 and, if c is increased still further, into the spiked solutions. This is shown in figure 9.

We can now draw, in figure 10, a fuller response diagram indicating the different types of periodic solutions.

The branches on the right of the diagram with few oscillations will coalesce when $c \approx 1$ when the spike at $t = \pi$ vanishes, but for n sufficiently large that $c_n \gg 1$ the amplitude of all the oscillations decays as G approaches $-u(t)$.

† The limitations of linear theory in discussing such high-frequency resonances have been discussed by Mortell & Seymour (1979).

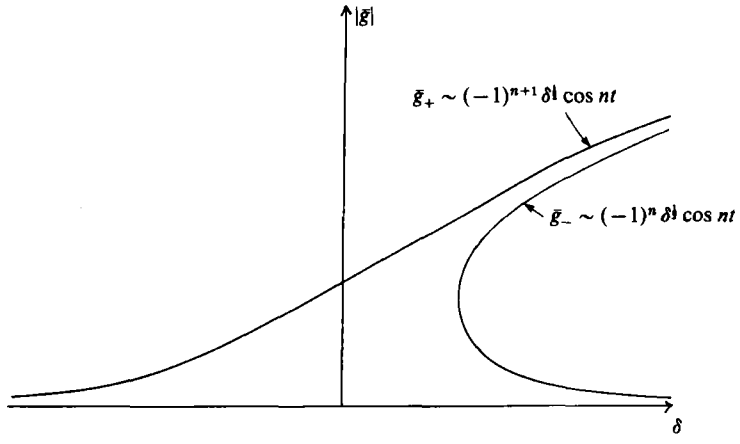

FIGURE 8. Response diagram for equation (12).

Some numerical solutions have been obtained which confirm this response diagram and enable us to fill in the curves for moderate values of n. The same numerical method (NAG D02BBF) was used to find even solutions of equation (2). The solution was found with $G(0) = \alpha$, $G'(0) = 0$ and α was varied until $|G'(\pi)| \leqslant 10^{-5}$. This gave the possible periodic solutions; several were found for each value of c and those for $c \approx 1.25$ are shown in figure 11. The procedure was repeated for other values of c, and

$$\lambda = \frac{3}{2\pi}\int_{-\pi}^{\pi} G\,\mathrm{d}t$$

was estimated from these graphs. It was then possible to fix some points on the response diagram in the (c, λ)-plane and sketch in the first of the curves. This is done in figure 12 for $\kappa = 0.54$, where the computed points are marked $\times$.

4. The effects of dissipation

As discussed in §2, dissipative effects may be introduced in several ways. The only model considered here introduces a small viscous term $\mu G'$ on the left-hand side of (2). This is more tractable than the integral form considered by Chester (1968) but probably less realistic.

The effect of dissipation on the phase plane of figure 3 is to change the closed orbits into spirals. The effect on the spiked solution is to make the spikes unsymmetrical, so that they no longer occur at the maximum and minimum values of u but are at points where u' is negative, as shown schematically in figure 13. The numerical and experimental solutions of Chester & Bones (1968) fit into this pattern, although they modelled the dissipation in a different way and their numerical method was based on a Fourier-series representation rather than an asymptotic expansion.

To see where these spikes can occur, we write the damped form of (2) in terms of the independent variable $\xi = f(t)/\kappa$ and the dependent variable $h(\xi) = G/u$ to obtain

$$\frac{f'^2}{u}\frac{\mathrm{d}^2h}{\mathrm{d}\xi^2} + \kappa\left(\frac{2u'f'}{u^2} + \frac{f''}{u} + \frac{\mu}{\kappa^2}\frac{f'}{u}\right)\frac{\mathrm{d}h}{\mathrm{d}\xi} + \kappa^2\left(\frac{u''}{u^2} + \frac{\mu}{\kappa^2}\frac{u'}{u^2}\right)h = \tfrac{2}{3}(h^2-1). \tag{13}$$

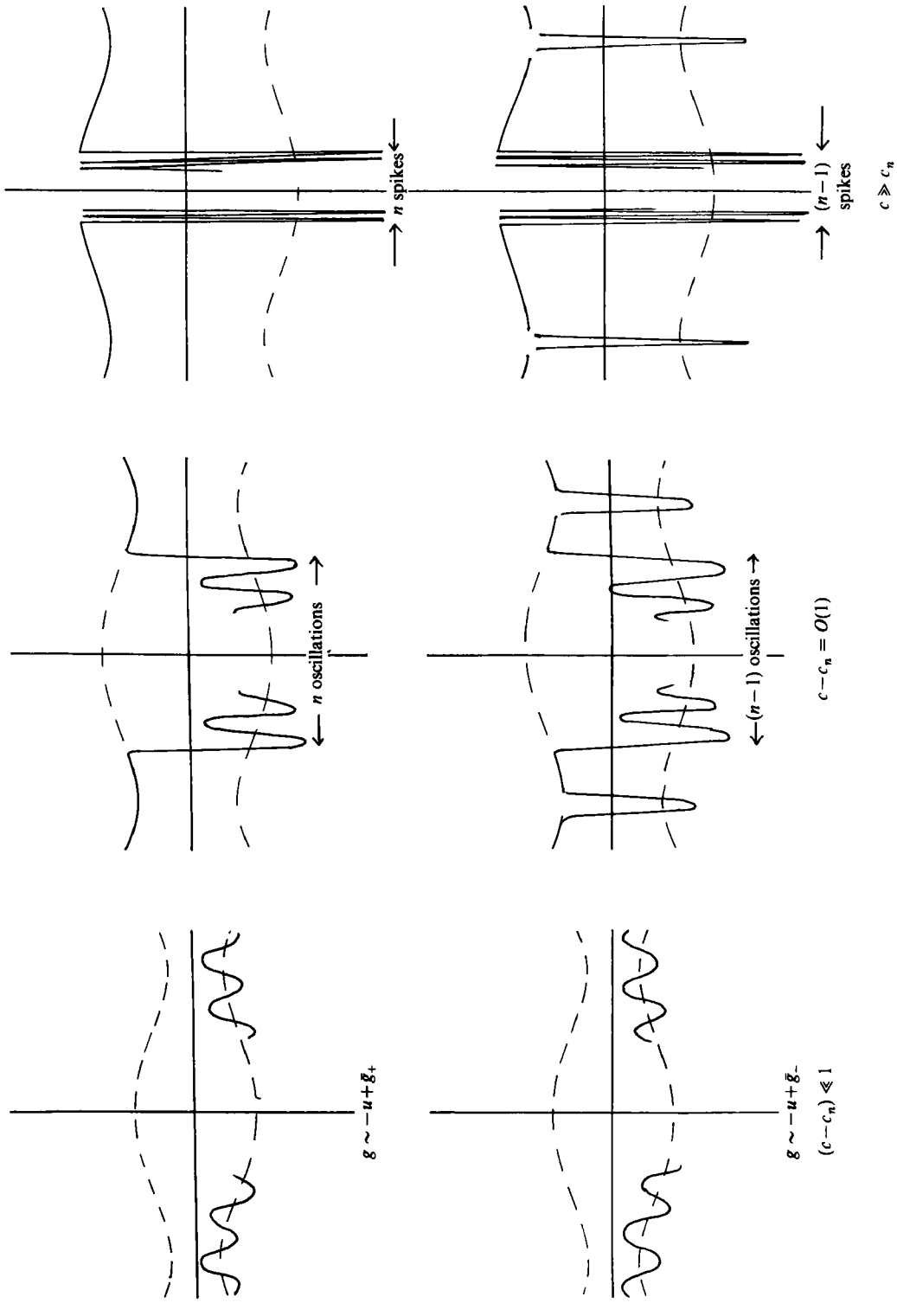

FIGURE 9. Evolution of solution branches as c increases.

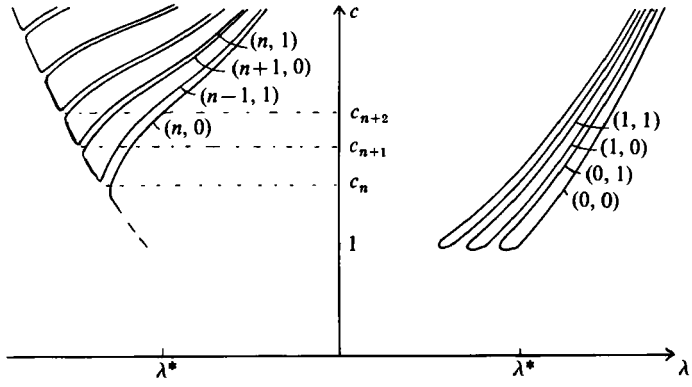

FIGURE 10. Response diagram for equation (12).

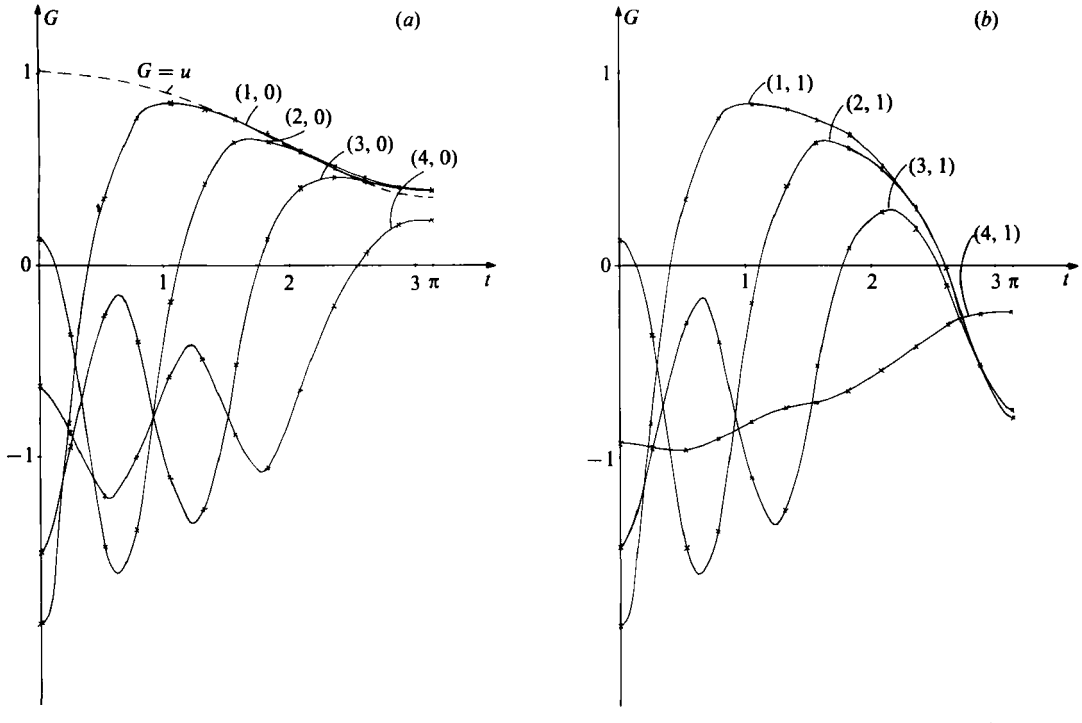

FIGURE 11. Numerical solutions of equation (2) when $\kappa = 0.54$ and $c = 1.2475 + 0.051\lambda$. (*a*) solutions with no spike at $t = \pi$; (*b*) solutions with a spike at $t = \pi$.

We choose $f' = u^{\frac{1}{2}}$ to make the first-order terms independent of u. Then, since $h \to 1$ as $\xi \to \pm\infty$, for a spike or a group of spikes near t we cannot have the damping term in equation (13) of one sign and so

$$\frac{2u'f'(t)}{u^2} + \frac{f''(t)}{u} + \frac{\mu}{\kappa^2}\frac{f'(t)}{u} = 0. \tag{14}$$

Putting $f' = u^{\frac{1}{2}}$ and $u = [(\frac{4}{3}\pi)(\cos t + c)]^{\frac{1}{2}}$, we see that (14) can only have a solution for t if $c < \hat{c} = [1 + (25\kappa^4/16\mu^2)]^{\frac{1}{2}}$.

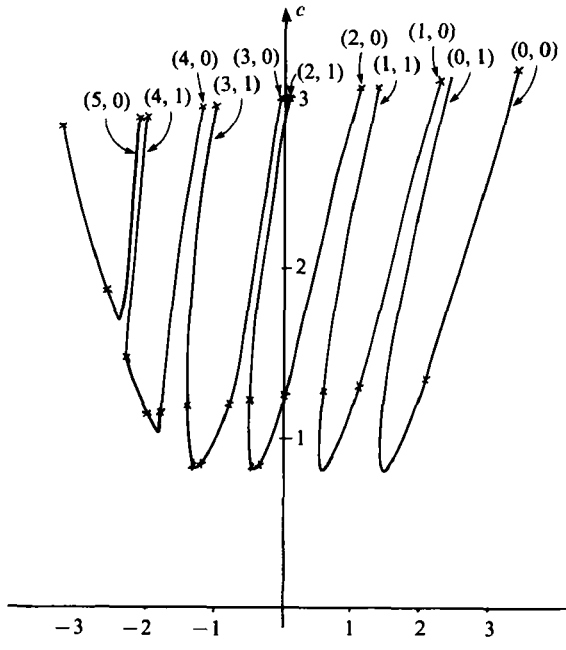

FIGURE 12. Response diagram for solutions of (2) obtained from numerical results when $\kappa = 0.54$.

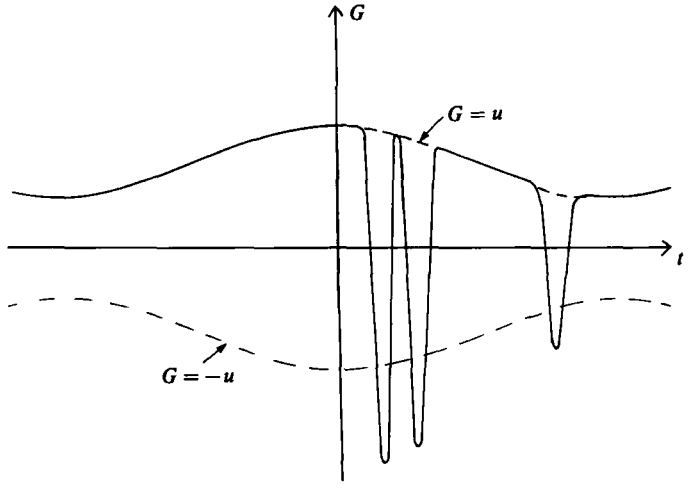

FIGURE 13. A spiked solution with damping.

When c is sufficiently close to 1 there are two values of t in $(0, \pi)$ satisfying (14). As c increases the spikes that were near $t = 0$ for the undamped case move to the right and the single spike at $t = \pi$ moves to the left. When $c = \hat{c}$ the two sets of spikes come together and there are no solutions of this type if $c > \hat{c}$. The response curves are shown schematically in figure 14. It should be noted that, although this response diagram cannot be compared directly with those of Chester & Bones (1968), since we have used a different amplitude parameter, it does give qualitatively the same

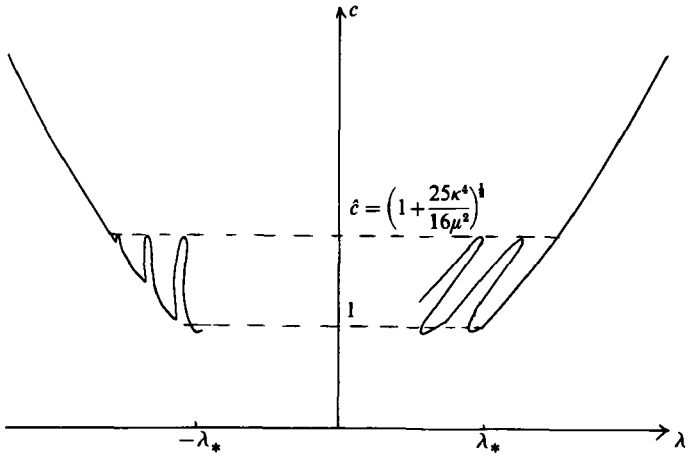

FIGURE 14. Response diagram for damped equation.

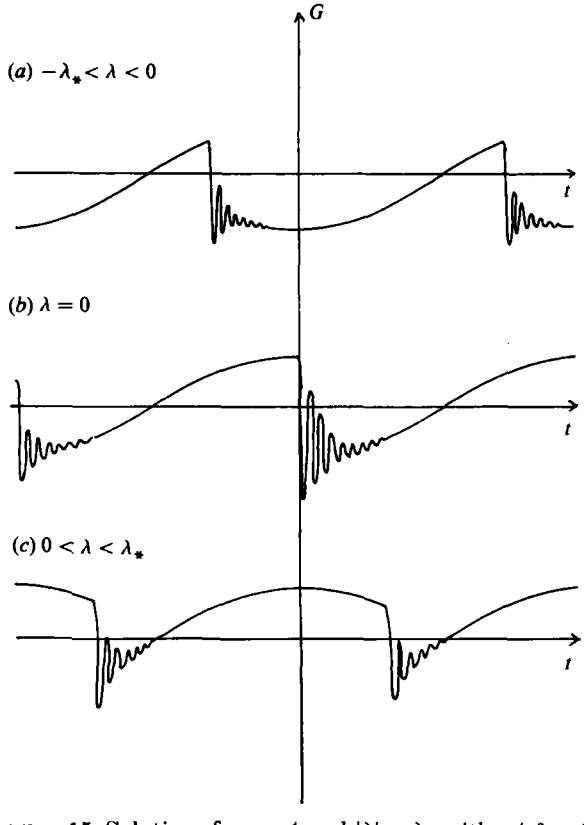

FIGURE 15. Solutions for $c = 1$ and $|\lambda| < \lambda_*$ with $\mu/\kappa^2 \gg 1$.

picture. This is true in spite of the different methods we have adopted for representing dissipation.

As μ increases (or κ decreases), $\hat{c}$ approaches 1, and solutions for $\lambda \in (-\lambda_*, \lambda_*)$ can only occur if c is very close to 1, and the response diagram approaches that which occurs in the dispersion-free case. The frequency of oscillations is high and so solutions will be as shown schematically in figure 15. These solutions may be compared with the shock solutions which are valid for $\kappa = 0$ in figure 1 (*b*).

5. Conclusion

We have presented asymptotic and numerical evidence that the response diagrams in figures 10 and 14 describe periodic sloshing in a shallow rectangular tank.

As the dispersion and damping are both decreased with $\kappa^2/\mu = O(1)$ the number of solution branches in the (c, λ)-plane (figure 10) increases indefinitely in the region above the dispersion-free response curve. Alternatively, if the damping is held constant while the dispersion parameter κ is decreased, the solutions approach the dispersion-free 'organ-pipe' resonant solutions as shown in figure 14. All our work has assumed the mean-square amplitude c is of order 1 and we have said nothing about the possibility of a very large amplitude response to a small forcing.

We are very grateful to W. Chester, S. Hastings, G. Keady, A. McNabb and F. N. Robinson for helpful discussions.

REFERENCES

CHESTER, W. 1964 *J. Fluid Mech.* **18**, 44.
CHESTER, W. 1968 *Proc. R. Soc. Lond.* A **306**, 5.
CHESTER, W. & BONES, J. A. 1968 *Proc. R. Soc. Lond.* A **306**, 23.
COX, E. A. & MORTELL, M. P. 1983 *Z. angew. Math. Phys.* **34**, 1.
COX, E. A. & MORTELL, M. P. 1986 *J. Fluid Mech.* **162**, 99.
HOLMES, P. & SPENCE, D. A. 1984 *Q. J. Mech. Appl. Maths* **37**, 525–538.
KATH, W. L. 1985 *Stud. Appl. Math.* **72**, 221.
KUZMAK, G. E. 1959 *Appl. Math. Mech.* **23**, 730.
LUKE, J. C. 1966 *Proc. R. Soc. Lond.* A **292**, 403.
MILES, J. W. 1985 *Wave Motion* **7**, 291–297.
MOISEYEV, N. N. 1958 *Prikl. Mat. Mech.* **22**, 612.
MORTELL, M. & SEYMOUR, B. R. 1979 *Proc. R. Soc. Lond.* A **367**, 253.
OCKENDON, J. R. & OCKENDON, H. 1973 *J. Fluid Mech.* **59**, 397.
VANDEN-BROECK, J.-M. 1984 *J. Fluid Mech.* **139**, 97.